THE JOURNAL OF PHYSICAL CHEMISTRY Letters

Letter

pubs.acs.org/JPCL

Tunneling Effect That Changes the Reaction Pathway from Epoxidation to Hydroxylation in the Oxidation of Cyclohexene by a Compound I Model of Cytochrome P450

Ranjana Gupta,[†] Xiao-Xi Li,[†,‡] Kyung-Bin Cho,[†] Mian Guo,[†] Yong-Min Lee,[†] Yong Wang,*[,‡] Shunichi Fukuzumi,*[,†,§] and Wonwoo Nam*[,†,‡]

[†]Department of Chemistry and Nano Science, Ewha Womans University, Seoul 03760, Korea

[‡]State Key Laboratory for Oxo Synthesis and Selective Oxidation, Suzhou Research Institute of LICP, Lanzhou Institute of Chemical Physics (LICP), Chinese Academy of Sciences, Lanzhou 730000, China

[§]Faculty of Science and Engineering, Meijo University, SENTAN, Japan Science and Technology Agency (JST), Nagoya, Aichi 468-8502, Japan

Supporting Information

ABSTRACT: The rate constants of the C=C epoxidation and the C−H hydroxylation (i.e., allylic C−H bond activation) in the oxidation of cyclohexene by a high-valent iron(IV)−oxo porphyrin π-cation radical complex, $[(TMP^{\bullet+})Fe^{IV}(O)(Cl)]$ (**1**, TMP = *meso*-tetramesitylporphyrin dianion), were determined at various temperatures by analyzing the overall rate constants and the products obtained in the cyclohexene oxidation by **1**, leading us to conclude that reaction pathway changes from the C=C epoxidation to C−H hydroxylation by decreasing reaction temperature. When cyclohexene was replaced by deuterated cyclohexene (cyclohexene-d_{10}), the epoxidation pathway dominated irrespective of the reaction temperature. The temperature dependence of the rate constant of the C−H hydroxylation pathway in the reactions of cyclohexene and cyclohexene-d_{10} by **1** suggests that there is a significant tunneling effect on the hydrogen atom abstraction of allylic C−H bonds of cyclohexene by **1**, leading us to propose that the tunneling effect is a determining factor for the switchover of the reaction pathway from the C=C epoxidation pathway to the C−H hydroxylation pathway by decreasing reaction temperature. By performing density functional theory (DFT) calculations, the reaction energy barriers of the C=C epoxidation and C−H bond activation reactions by **1** were found to be similar, supporting the notion that small environmental changes, such as the reaction temperature, can flip the preference for one reaction to another.

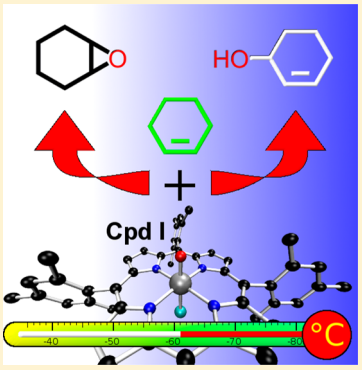

High-valent iron(IV)−oxo porphyrin π-cation radical species, called Compound I (Cpd I), have been spectroscopically characterized and well accepted as reactive intermediates in the catalytic cycles of heme enzymes, such as cytochrome P450 (P450), horseradish peroxidase (HRP), catalase, and chloroperoxidase.[1−8] Biomimetic studies using synthetic iron porphyrin complexes have provided valuable insights into the reactivities and reaction mechanisms of the intermediates in various oxidation reactions as well as in electron-transfer reactions.[9−22] For example, it has been reported that the regioselectivity of C=C epoxidation versus C−H hydroxylation in the oxidation of cyclohexene by Cpd I models changes dramatically depending on reaction temperatures, substrates, and the electronic nature of iron porphyrins.[23,24] However, activation parameters of the rate constants of the C=C epoxidation versus the C−H hydroxylation of the same substrate, including the deuterium kinetic isotope effect (KIE), has yet to be clarified in comparison with density functional theory (DFT) calculations. In addition, factors that determine the reaction pathways (e.g., C=C epoxidation versus C−H hydroxylation) in the oxidation of cyclohexene by Cpd I models need to be clarified, although we have discussed recently the regioselectivity switch (e.g., C=C epoxidation versus C−H hydroxylation) in the oxidation of cyclic olefins by nonheme metal(IV)−oxo complexes,[25−29] and Shaik and co-workers have shown the tunneling effect on the counterintuitive hydrogen atom (H atom) abstraction reactivity of nonheme iron(IV)−oxo complexes.[30,31]

We report herein the temperature effect on the rate constants of the C=C epoxidation and C−H hydroxylation pathways in the oxidation of cyclohexene and deuterated cyclohexene (cyclohexene-d_{10}) by a Cpd I model compound by determining both the overall rate constants and products at various reaction temperatures. The switchover of the reaction pathway from the C=C epoxidation to the C−H hydroxylation in the oxidation of cyclohexene by a Cpd I model compound was observed by decreasing the reaction temperature. The temperature dependence of the deuterium KIE revealed the significance of the

Received: February 25, 2017
Accepted: March 16, 2017
Published: March 16, 2017

DOI: 10.1021/acs.jpclett.7b00461
J. Phys. Chem. Lett. 2017, 8, 1557−1561

tunneling effect on the H atom abstraction step in the hydroxylation of cyclohexene, resulting in the switchover of the reaction pathway from C=C epoxidation to C−H hydroxylation by decreasing the reaction temperature. This experimental observation was corroborated by DFT calculations.

An iron(IV)−oxo porphyrin π-cation radical complex, $[(TMP^{\bullet+})Fe^{IV}(O)(Cl)]$ (**1**, TMP = *meso*-tetramesitylporphyrin dianion), was prepared by reacting $[(TMP)Fe^{III}(Cl)]$ with 2 equiv of *m*-chloroperbenzoic acid (*m*-CPBA) in butyronitrile (C_3H_7CN) at 193 K (see Supporting Information (SI), Figures S1 and S2 for the UV−vis absorption and EPR spectra of **1**).[23,24,29] Upon addition of cyclohexene to a C_3H_7CN solution of **1** at 193 K, the absorption band at 666 nm due to **1** decayed with an increase in the absorption band at 507 nm due to $[(TMP)Fe^{III}(Cl)]$ (Figure 1a). The decay time profile of absorbance at 666 nm due to **1** obeyed first-order kinetics (Figure 1a, inset). The first-order rate constant (k_{obs}) was proportional to the concentration of cyclohexene (Figure 1b), and a second-order rate constant ($k_{2(H)}$) was determined to be 0.42 M^{-1} s^{-1} at 193 K from the slope of the linear plot of the first-order rate constants vs concentrations of cyclohexene (Figure 1b). Similarly, the $k_{2(H)}$ values at different temperatures were determined from the slopes of the linear plots of the first-order rate constants vs concentrations of cyclohexene (Table 1; Figure 1b and SI, Figures S3−S6). When cyclohexene (10 mM) was replaced by cyclohexene-d_{10} (10 mM), the decay rate constant of **1** with cyclohexene-d_{10} (1.7×10^{-3} s^{-1} at 193 K) became smaller than that of **1** with cyclohexene (4.3×10^{-3} s^{-1} at 193 K) (Figure 1a, inset). The $k_{2(D)}$ values in the oxidation of cyclohexene-d_{10} by **1** at various temperatures were also determined from the slopes of the linear plots of the first-order rate constants vs concentrations of cyclohexene-d_{10} (Table 1; Figure 1b and SI, Figures S3−S6).

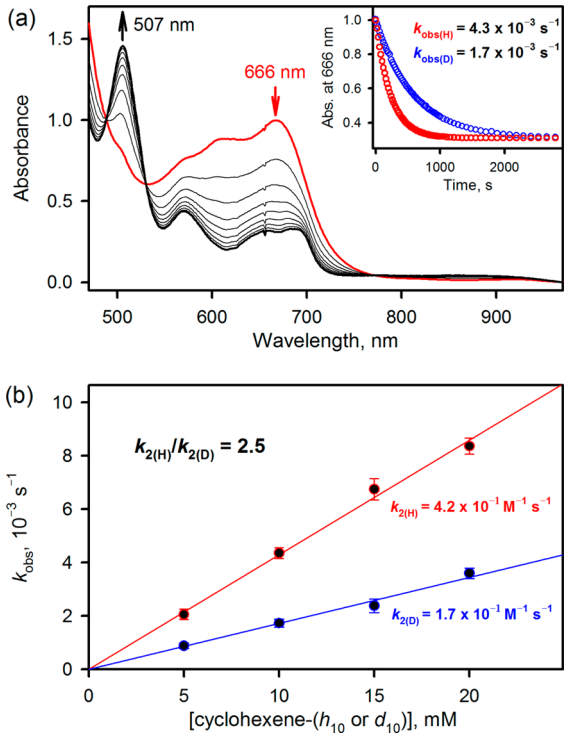

Figure 1. (a) UV−vis absorption spectral changes observed in the oxidation of cyclohexene (10 mM) by **1** (0.10 mM) in C_3H_7CN at 193 K. Insets show the time courses (red circles for cyclohexene and blue circles for cyclohexene-d_{10}) monitored for the absorbance change at 666 nm due to **1**. (b) Plots of pseudo-first-order rate constants (k_{obs}) vs concentrations of cyclohexene (red) and cyclohexene-d_{10} (blue) in the oxidation of cyclohexene and cyclohexene-d_{10} by **1** (0.10 mM) in C_3H_7CN at 193 K.

The products in the oxidation of cyclohexene and cyclohexene-d_{10} by **1** were analyzed to be cyclohexene oxide and cyclohex-2-enol (see SI, Experimental Section), and the product yields at different temperatures are summarized in Table 2. The ratio of the epoxide to alcohol products in the oxidation of cyclohexene by **1** decreased with decreasing reaction temperature, such that the ratio became almost unity at 213 K and reversed at lower temperatures. In contrast to this, the product ratio of the epoxide to the alcohol products in the oxidation of cyclohexene-d_{10} slightly increased with decreasing reaction temperature. The cyclohexene oxide was the predominant product at the lower temperature (i.e., 193 K).

Table 2. Product Yields in the Reactions of 1 (0.10 mM) with Cyclohexene and Cyclohexene-d_{10} in C_3H_7CN at Various Temperatures

	cyclohexene-h_{10} product yields (%)		cyclohexene-d_{10} product yields (%)	
temp. (K)	cyclohexene oxide	cyclohex-2-enol	cyclohexene oxide	cyclohex-2-enol
233	65(5)	27(3)	64(4)	19(3)
223	54(5)	38(4)	72(5)	16(2)
213	45(4)	47(5)	78(4)	13(3)
203	36(3)	55(4)	82(4)	12(3)
193	34(4)	62(4)	84(4)	12(2)

Because the observed second-order rate constant ($k_{2(H)}$) of the oxidation of cyclohexene by **1** corresponds to the sum of the rate constants of epoxidation ($k_{O(H)}$) and hydroxylation (k_H), $k_{2(H)} = k_{O(H)} + k_H$, the $k_{O(H)}$ and k_H values were determined from the $k_{2(H)}$ values (Table 1) and the product ratios of the epoxide to the alcohol products (Table 2). Similarly, the $k_{O(D)}$ and k_D values of cyclohexene-d_{10} were

Table 1. Rate Constants of Epoxidation (k_O) and Hydroxylation of Cyclohexene (k_H) and Cyclohexene-d_{10} (k_D) with 1 in C_3H_7CN at Various Temperatures

	cyclohexene-h_{10}			cyclohexene-d_{10}			KIE	
temp. (K)	$k_{2(H)}$ (M^{-1} s^{-1})	$k_{O(H)}$ (M^{-1} s^{-1})	k_H (M^{-1} s^{-1})	$k_{2(D)}$ (M^{-1} s^{-1})	$k_{O(D)}$ (M^{-1} s^{-1})	k_D (M^{-1} s^{-1})	$k_{O(H)}/k_{O(D)}$	k_H/k_D
233	12(1)	8.5	3.5	11(1)	8.5	2.5	1.0	1.4
223	5.0(4)	2.9	2.1	3.5(3)	2.9	0.64	1.0	3.3
213	2.0(2)	0.98	1.0	1.1(1)	0.94	0.16	1.0	6.3
203	0.70(5)	0.28	0.42	0.31(3)	0.27	0.040	1.0	11
193	0.42(4)	0.15	0.27	0.17(2)	0.15	0.021	1.0	13

DOI: 10.1021/acs.jpclett.7b00461
J. Phys. Chem. Lett. 2017, 8, 1557−1561

determined from the $k_{2(D)}$ values (Table 1) and the product ratios (Table 2). It should be noted that the $k_{O(H)}$ values obtained from the reaction of cyclohexene were virtually identical to the $k_{O(D)}$ values obtained from the reaction of cyclohexene-d_{10}, and thus, there is no deuterium KIE on the epoxidation of cyclohexene by **1** (i.e., KIE = $k_{O(H)}/k_{O(D)}$ = 1.0; see Table 1). In contrast to the C=C epoxidation, the KIE values obtained in the hydroxylation of cyclohexene and cyclohexene-d_{10} were different depending on reaction temperatures and the KIE values increased with decreasing reaction temperature (Table 1, column of k_H/k_D).

Arrhenius plots of the rate constants of the epoxidation ($k_{O(H)} = k_{O(D)}$) and the hydroxylation of cyclohexene (k_H) and cyclohexene-d_{10} (k_D) by **1** in C_3H_7CN are shown in Figure 2,

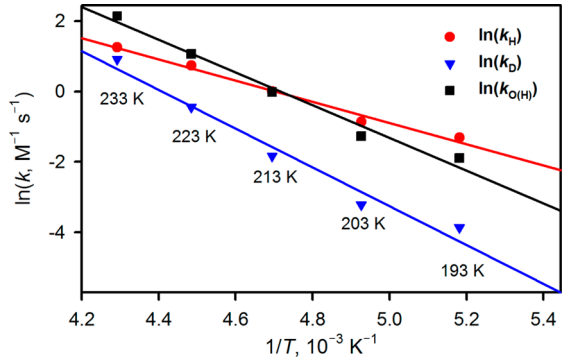

Figure 2. Arrhenius plots of the rate constants of epoxidation ($k_{O(H)}$) and hydroxylation of cyclohexene-h_{10} (k_H) and cyclohexene-d_{10} (k_D) by [(TMP$^{\bullet+}$)Fe^{IV}(O)(Cl)] (**1**) in C_3H_7CN.

where the activation energy of the epoxidation of cyclohexene and cyclohexene-d_{10} ($E_{O(H)} \approx E_{O(D)}$ = 9.3 kcal mol^{-1}) is similar to that of hydroxylation of cyclohexene-d_{10} (E_D = 11 kcal mol^{-1}) but is significantly higher than that of hydroxylation of cyclohexene (E_H = 6.0 kcal mol^{-1}). As a result, there is a crossing point between $k_{O(H)}$ and k_H at around 213 K, where $k_{O(H)}$ is the same as k_H. The $k_{O(H)}$ value is larger than the corresponding k_H value at the higher temperatures, above 213 K, whereas the k_H value is larger than the corresponding $k_{O(H)}$ value at the lower temperatures, below 213 K. Thus, a switchover of the reaction pathways between C=C epoxidation and C−H hydroxylation of cyclohexene by **1** occurs depending on the reaction temperature. The pre-exponential factor (A_H) of hydroxylation of cyclohexene (1.5×10^6 M^{-1} s^{-1}) is significantly smaller than the corresponding value of cyclohexene-d_{10} ($A_D = 3.5 \times 10^{10}$ M^{-1} s^{-1}). Such a large difference in the pre-exponential factor ($A_D \gg A_H$) together with a large difference in the activation energies ($E_D - E_H$ = 5.0 kcal mol^{-1}), which is larger than that expected from the difference in the bond dissociation energy between C−H and C−D (BDE$_D$ − BDE$_H$ = 1.3 kcal mol^{-1}), results from a tunneling effect.[32−34] Because it is the curvature of the Arrhenius plot that demonstrates experimentally the incidence of tunneling, the tunneling has been detected with two distinctive findings of $E_D \gg E_H$ and $A_D \gg A_H$.[32−34]

The reaction rate constants in Table 1 can be translated into free energy barriers through the Eyring equation, resulting in the C=C epoxidation and C−H hydroxylation free energy barriers being in the ranges of 11.8−12.5 and 11.6−12.9 kcal mol^{-1}, respectively, depending on the reaction temperature. These energy ranges, which are within 1.3 kcal mol^{-1}, pose a challenge for DFT calculations as the error margins are typically larger than that. Therefore, a successful calculation would be if the results showed that the epoxidation energy barrier is not too much different from the hydroxylation reaction barrier as this will support the experiments showing that the reaction pathway can be changed by changing external factors (i.e., the temperature). With this goal set, we performed the DFT calculations for both C=C epoxidation and C−H hydroxylation reactions in the oxidation of cyclohexene by the Cpd I model (SI, Tables S1−S5).

We use the electronic energies (including solvent and dispersion effects) here due to a presumed higher accuracy rather than free energies (see the SI for discussion). The S = 1/2 and 3/2 spin states of Cpd I are found to be energetically degenerate within round-off errors (Figure 3, center). The

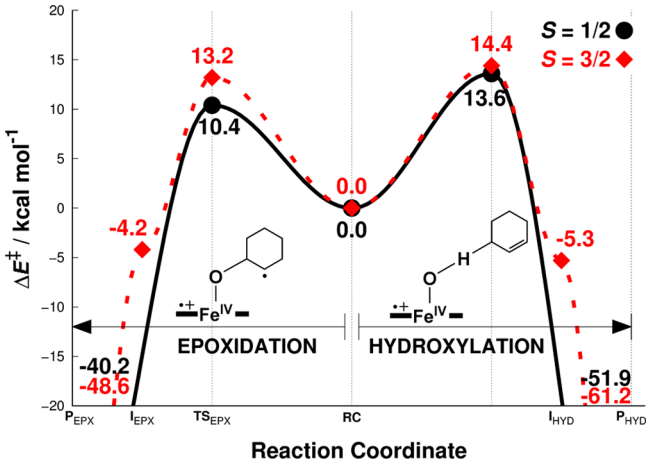

Figure 3. DFT-calculated reaction energy barriers for the oxidation reactions of cyclohexene by **1** at the B3LYP/LACV3P+*//LACVP level including dispersion and solvent effects.

energies and spin state distribution are in accord with earlier findings on Cpd I and feature an α or β unpaired electron on the porphyrin ligand, depending on the spin state.[35] The calculated electronic energies show that the epoxidation S = 1/2 low-spin barrier is the lowest at 10.4 kcal mol^{-1} and involve an initial β-electron transfer from the substrate to the Fe^{IV}O moiety.[36] The S = 3/2 epoxidation barrier is slightly higher at 13.2 kcal mol^{-1}. The hydroxylation barriers on the other hand are even higher, at 13.6 and 14.4 kcal mol^{-1} for S = 1/2 and S = 3/2 spin states, respectively. Both high-spin pathways feature an intermediate state after the transition state where the substrate is in a radical state (see the SI section High-Spin Intermediates in the Reactions for a more in-depth discussion about these intermediates), before the intermediate proceeds to the product with a low or no energy barrier. Such a stable intermediate state was not found for the low-spin pathway.

The calculation results imply that the C=C epoxidation pathway is preferred to the hydroxylation pathway by 3.2 kcal mol^{-1}, which is in agreement with the experimental results described above except at the very low temperature. The difference in the value of 3.2 kcal mol^{-1} is sufficiently small and implies that a hydroxylation reaction can be achieved if conditions are favorable for it, such as at a low temperature in which the tunneling effect becomes relatively more important than other effects due to its insensitivity to changing temperature.

DOI: 10.1021/acs.jpclett.7b00461
J. Phys. Chem. Lett. 2017, 8, 1557−1561

In conclusion, a switchover of the reaction pathway from the C=C epoxidation to the C−H hydroxylation was observed in the oxidation of cyclohexene by a Cpd I model compound, $[(TMP^{\bullet+})Fe^{IV}(O)(Cl)]$ (**1**), by lowering the reaction temperature only. This was deemed to be due to the tunneling effect on the H atom abstraction for the hydroxylation pathway; the KIE values in the hydroxylation pathway increased with decreasing reaction temperature. Such a switchover of the reaction pathways between the C=C epoxidation and the C−H hydroxylation in the oxidation of cyclohexene by the Cpd I model compound depending on reaction temperature was further supported by DFT calculations, in which the C=C epoxidation reaction has a lower energy barrier than the H atom transfer step in the C−H hydroxylation reaction at ambient temperature, but the H atom transfer step can become the preferable pathway at low temperature, resulting from the tunneling effect. Such a tunneling effect has never been considered as a factor to switch the reaction pathway previously. Thus, the present study has demonstrated for the first time the importance of the tunneling effect, especially at low reaction temperature, in the H atom transfer step in the C−H hydroxylation pathway, which is in competition with the epoxidation pathway, in the oxidation of cyclohexene by high-valent iron(IV)−oxo porphyrin π-cation radical species (Cpd I).

■ ASSOCIATED CONTENT

Supporting Information

The Supporting Information is available free of charge on the ACS Publications website at DOI: 10.1021/acs.jpclett.7b00461.

Figures S1−S6, Tables S1−S5, experimental and DFT calculation sections, and DFT coordinates (PDF)

■ AUTHOR INFORMATION

Corresponding Authors

*E-mail: wangyong@licp.cas.cn (Y.W.).
*E-mail: fukuzumi@chem.eng.osaka-u.ac.jp (S.F.).
*E-mail: wwnam@ewha.ac.kr (W.N.).

ORCID

Kyung-Bin Cho: 0000-0001-6586-983X
Shunichi Fukuzumi: 0000-0002-3559-4107
Wonwoo Nam: 0000-0001-8592-4867

Notes

The authors declare no competing financial interest.

■ ACKNOWLEDGMENTS

The authors acknowledge financial support from the NRF of Korea through the CRI (NRF-2012R1A3A2048842 to W.N.), GRL (NRF-2010-00353 to W.N.) and MSIP (NRF-2013R1A1A2062737 to K.-B.C.) and from JSPS KAKENHI (No. 16H02268 to S.F.).

■ REFERENCES

(1) McQuarters, A. B.; Wolf, M. W.; Hunt, A. P.; Lehnert, N. 1958−2014: After 56 Years of Research, Cytochrome P450 Reactivity Is Finally Explained. *Angew. Chem., Int. Ed.* **2014**, *53*, 4750−4752.

(2) Shoji, O.; Watanabe, Y. Peroxygenase Reactions Catalyzed by Cytochromes P450. *J. Biol. Inorg. Chem.* **2014**, *19*, 529−539.

(3) Krest, C. M.; Onderko, E. L.; Yosca, T. H.; Calixto, J. C.; Karp, R. F.; Livada, J.; Rittle, J.; Green, M. T. Reactive Intermediates in Cytochrome P450 Catalysis. *J. Biol. Chem.* **2013**, *288*, 17074−17081.

(4) de Visser, S. P. Predictive Studies of Oxygen Atom Transfer Reactions by Compound I of Cytochrome P450: Aliphatic and Aromatic Hydroxylation, Epoxidation, and Sulfoxidation. *Adv. Inorg. Chem.* **2012**, *64*, 1−31.

(5) Jung, C.; de Vries, S.; Schünemann, V. Spectroscopic Characterization of Cytochrome P450 Compound I. *Arch. Biochem. Biophys.* **2011**, *507*, 44−55.

(6) Hersleth, H.-P.; Ryde, U.; Rydberg, P.; Görbitz, C. H.; Andersson, K. K. Structures of the High-Valent Metal-Ion Haem-Oxygen Intermediates in Peroxidases, Oxygenases and Catalases. *J. Inorg. Biochem.* **2006**, *100*, 460−476.

(7) Nicholls, P. Classical Catalase: Ancient and Modern. *Arch. Biochem. Biophys.* **2012**, *525*, 95−101.

(8) Rittle, J.; Green, M. T. Cytochrome P450 Compound I: Capture, Characterization, and C-H Bond Activation Kinetics. *Science* **2010**, *330*, 933−937.

(9) Oszajca, M.; Franke, A.; Brindell, M.; Stochel, G.; van Eldik, R. Redox Cycling in the Activation of Peroxides by Iron Porphyrin and Manganese Complexes. 'Catching' Catalytic Active Intermediates. *Coord. Chem. Rev.* **2016**, *306*, 483−509.

(10) Lindhorst, A. C.; Haslinger, S.; Kühn, F. E. Molecular Iron Complexes as Catalysts for Selective C-H Bond Oxygenation Reactions. *Chem. Commun.* **2015**, *51*, 17193−17212.

(11) Ryabov, A. D. Green Challenges of Catalysis via Iron(IV)oxo and Iron(V)oxo Species. *Adv. Inorg. Chem.* **2013**, *65*, 117−163.

(12) Costas, M. Selective C-H Oxidation Catalyzed by Metalloporphyrins. *Coord. Chem. Rev.* **2011**, *255*, 2912−2932.

(13) Che, C.-M.; Lo, V. K.-Y.; Zhou, C.-Y.; Huang, J.-S. Selective Functionalisation of Saturated C-H Bonds with Metalloporphyrin Catalysts. *Chem. Soc. Rev.* **2011**, *40*, 1950−1975.

(14) Gunay, A.; Theopold, K. H. C-H Bond Activations by Metal Oxo Compounds. *Chem. Rev.* **2010**, *110*, 1060−1081.

(15) Shaik, S.; Cohen, S.; Wang, Y.; Chen, H.; Kumar, D.; Thiel, W. P450 Enzymes: Their Structure, Reactivity, and Selectivity-Modeled by QM/MM Calculations. *Chem. Rev.* **2010**, *110*, 949−1017.

(16) Che, C.-M.; Huang, J.-S. Metalloporphyrin-Based Oxidation Systems: From Biomimetic Reactions to Application in Organic Synthesis. *Chem. Commun.* **2009**, 3996−4015.

(17) Mansuy, D. A Brief History of the Contribution of Metalloporphyrin Models to Cytochrome P450 Chemistry and Oxidation Catalysis. *C. R. Chim.* **2007**, *10*, 392−413.

(18) Zhou, X.; Chen, X.; Jin, Y.; Markó, I. E. Evidence of Two Key Intermediates Contributing to the Selectivity of P450 Biomimetic Oxidation of Sulfides to Sulfoxides and Sulfones. *Chem. - Asian J.* **2012**, *7*, 2253−2257.

(19) Fukuzumi, S. Electron-Transfer Properties of High-Valent Metal-Oxo Complexes. *Coord. Chem. Rev.* **2013**, *257*, 1564−1575.

(20) Shaik, S.; Hirao, H.; Kumar, D. Reactivity of High-Valent Iron-Oxo Species in Enzymes and Synthetic Reagents: A Tale of Many States. *Acc. Chem. Res.* **2007**, *40*, 532−542.

(21) Nam, W. High-Valent Iron(IV)-Oxo Complexes of Heme and Non-Heme Ligands in Oxygenation Reactions. *Acc. Chem. Res.* **2007**, *40*, 522−531.

(22) Ji, L.; Franke, A.; Brindell, M.; Oszajca, M.; Zahl, A.; van Eldik, R. Combined Experimental and Theoretical Study on the Reactivity of Compounds I and II in Horseradish Peroxidase Biomimetics. *Chem. - Eur. J.* **2014**, *20*, 14437−14450.

(23) Song, W. J.; Ryu, Y. O.; Song, R.; Nam, W. Oxoiron(IV) Porphyrin p-Cation Radical Complexes with a Chameleon Behavior in Cytochrome P450 Model Reactions. *J. Biol. Inorg. Chem.* **2005**, *10*, 294−304.

(24) Nam, W.; Lim, M. H.; Oh, S.-Y.; Lee, J. H.; Lee, H. J.; Woo, S. K.; Kim, C.; Shin, W. Remarkable Anionic Axial Ligand Effects of Iron(III) Porphyrin Complexes on the Catalytic Oxygenations of Hydrocarbons by H_2O_2 and the Formation of Oxoiron(IV) Porphyrin Intermediates by *m*-Chloroperoxybenzoic Acid. *Angew. Chem., Int. Ed.* **2000**, *39*, 3646−3649.

(25) Kwon, Y. H.; Mai, B. K.; Lee, Y.-M.; Dhuri, S. N.; Mandal, D.; Cho, K.-B.; Kim, Y.; Shaik, S.; Nam, W. Determination of Spin

DOI: 10.1021/acs.jpclett.7b00461
J. Phys. Chem. Lett. 2017, 8, 1557−1561

Inversion Probability, H-Tunneling Correction, and Regioselectivity in the Two-State Reactivity of Nonheme Iron(IV)-Oxo Complexes. *J. Phys. Chem. Lett.* **2015**, *6*, 1472−1476.
(26) Dhuri, S. N.; Cho, K.-B.; Lee, Y.-M.; Shin, S. Y.; Kim, J. H.; Mandal, D.; Shaik, S.; Nam, W. Interplay of Experiment and Theory in Elucidating Mechanisms of Oxidation Reactions by a Nonheme $Ru^{IV}O$ Complex. *J. Am. Chem. Soc.* **2015**, *137*, 8623−8632.
(27) Kim, S.; Cho, K.-B.; Lee, Y.-M.; Chen, J.; Fukuzumi, S.; Nam, W. Factors Controlling the Chemoselectivity in the Oxidation of Olefins by Nonheme Manganese(IV)-Oxo Complexes. *J. Am. Chem. Soc.* **2016**, *138*, 10654−10663.
(28) Bae, S. H.; Seo, M. S.; Lee, Y.-M.; Cho, K.-B.; Kim, W.-S.; Nam, W. Mononuclear Nonheme High-Spin (S = 2) versus Intermediate-Spin (S = 1) Iron(IV)-Oxo Complexes in Oxidation Reactions. *Angew. Chem., Int. Ed.* **2016**, *55*, 8027−8031.
(29) Kumar, D.; Tahsini, L.; de Visser, S. P.; Kang, H. Y.; Kim, S. J.; Nam, W. Effect of Porphyrin Ligands on the Regioselective Dehydrogenation versus Epoxidation of Olefins by Oxoiron(IV) Mimics of Cytochrome P450. *J. Phys. Chem. A* **2009**, *113*, 11713−11722.
(30) Mandal, D.; Ramanan, R.; Usharani, D.; Janardanan, D.; Wang, B.; Shaik, S. How Does Tunneling Contribute to Counterintuitive H-Abstraction Reactivity of Nonheme Fe(IV)O Oxidants with Alkanes? *J. Am. Chem. Soc.* **2015**, *137*, 722−733.
(31) Mandal, D.; Shaik, S. Interplay of Tunneling, Two-State Reactivity, and Bell-Evans-Polanyi Effects in C-H Activation by Nonheme Fe(IV)O Oxidants. *J. Am. Chem. Soc.* **2016**, *138*, 2094−2097.
(32) Kwart, H. Temperature Dependence of the Primary Kinetic Hydrogen Isotope Effect as a Mechanistic Criterion. *Acc. Chem. Res.* **1982**, *15*, 401−408.
(33) Fukuzumi, S.; Kobayashi, T.; Suenobu, T. Unusually Large Tunneling Effect on Highly Efficient Generation of Hydrogen and Hydrogen Isotopes in pH-Selective Decomposition of Formic Acid Catalyzed by a Heterodinuclear Iridium-Ruthenium Complex in Water. *J. Am. Chem. Soc.* **2010**, *132*, 1496−1497.
(34) Lewandowska-Andralojc, A.; Grills, D. C.; Zhang, J.; Bullock, R. M.; Miyazawa, A.; Kawanishi, Y.; Fujita, E. Kinetic and Mechanistic Studies of Carbon-to-Metal Hydrogen Atom Transfer Involving Os-Centered Radicals: Evidence for Tunneling. *J. Am. Chem. Soc.* **2014**, *136*, 3572−3578.
(35) Shaik, S.; Kumar, D.; de Visser, S. P.; Altun, A.; Thiel, W. Theoretical Perspective on the Structure and Mechanism of Cytochrome P450 Enzymes. *Chem. Rev.* **2005**, *105*, 2279−2328.
(36) Conventional wisdom dictates that a Cpd I reduction reaction occurs preferentially through an α-electron transfer to the porphyrin ligand. In this case, however, after a thorough investigation, we are confident that this is a β-electron transfer to the $Fe^{IV}O$ moiety instead, and details will be communicated separately in the near future.

DOI: 10.1021/acs.jpclett.7b00461
J. Phys. Chem. Lett. 2017, 8, 1557−1561